Numerical Analysis of Laminar Flame Speed for H_2-NH_3-Air mixtures in Premixed Jet Flames

Peyman Zahedi[*] and Kianoosh Yousefi[**, §]

[*] Department of Mechanical Engineering, Mashhad Branch, Islamic Azad University, Mashhad, Iran
[**] Department of Mechanical Engineering, Mashhad Branch, Islamic Azad University, Mashhad, Iran

([§]Correspondent author's E-mail: kianoosh_py@yahoo.com)

ABSTRACT: A numerical study of laminar flame speeds for premixed H_2-NH_3-air jet flames is carried out for 0 to 80% NH_3 in H_2 for different equivalence ratios from lean to rich conditions. Flame-speed predictions have been conducted by CHEMKIN package over a wide range of conditions. These data are then used to validate by experimental flame speeds in literature. The results demonstrated that these mechanisms perform well for H_2-air combustion. Differences in flame speeds and associated radical species concentrations (H, O, and OH) are found to be largest for higher levels of NH_3 and with increasing equivalence ratio. It is also revealed that OH is the key radical leading to NH_3 decomposition and is a likely source of deviation between model predictions. The numerical data show that GRI-Mech 3.0 mechanism is the capable of accurately projecting reductions in flame speed as much as 90 to 95% with NH_3 addition.

Keywords: Laminar Flame Speed, Premixed Flames, Ammonia, Hydrogen.

INTRODUCTION

The growing demand for viable alternative fuels with reduced pollutant has drawn significant attention towards hydrogen (H_2) combustion for heating, power, and transportation. However, there are still primary obstacles associated with hydrogen storage and distribution, leading to a wide range of research efforts that have suggested ammonia (NH_3) as a potential alternative fuel (Zamfirescu and Dincer, 2009). Ammonia is typically generated using the Haber-Bosch process, and it can also be generated via electrolysis of water from renewable sources. Once produced, NH_3 is a carbon-free fuel with a higher energy density than liquid H_2 and can easily be stored as a liquid at a pressure of about 8 bar at 21 °C, making it an ideal H_2 carrier. By comparison, liquid H_2 requires several hundred bar for effective storage.

Considering the potential for NH_3 to serve as an alternative fuel or as an H_2 carrier, a number of studies have investigated the flame stability and emissions characteristics of NH_3 for combustors or engine applications. This includes the combustion of pure NH_3 as well as NH_3 mixed with conventional fuels such as H_2 and methane (CH_4), among others (Miller and Bowman, 1989 and Bian, 1991). Reiter and Kong [2011], showed that NH_3 could replace 95% of the diesel fuel in a conventional diesel engine and reduce NO_x emissions. Similarly, the effects of NH_3 substitution to improve the safety and performance of H_2 internal combustion engines were investigated and compared with results from computational modelling (Lee et al., 2010), which these studies show that NH_3 can potentially act as an alternative fuel. Recently, Mendiara and Glarborg, 2009, have extended a chemical kinetics model involving 97 species and 779 reactions for the oxidation of NH_3 in oxy-fuel combustion of CH_4/NH_3 in

a laminar flow reactor, which captured experimental trends fairly well. Furthermore, Konnov, 2009, as well as Tian et al., 2009, have developed chemical mechanisms for hydrocarbon/NH_3 and H_2/NH_3 reactions in a companion research with that of Mendiara and Glarborg. Compared with the Miller and Bowman, these mechanisms have been expanded with more extensive reactions for NH_3 chemistry.

The Konnov mechanism was found to be in agreement with the measured NO concentrations in lean CH_4–NH_3–air premixed flames, but NO lean re-burning was not well predicted. Duynslaegher et al., 2009, utilized the Konnov mechanism to investigate the effects of initial H_2 content on NH_3–H_2–O_2–Ar flames. They were able to predict the effects of equivalence ratio on NO formation but found disagreement for NH_2 and N_2O species concentrations. Later, Shmakov et al., 2010, studied NO- and NH_3-doped H_2–O_2–N_2 flames experimentally and numerically using a derivative of the Konnov detailed reaction mechanism and provided modifications to the reaction chemistry based on the experimental data for better overall agreement. Tian et al., 2009, proposed a comprehensive kinetics mechanism based on the experimental and modeling study of 11 premixed NH3/CH4/O2/Ar flames at low-pressure, stoichiometric conditions. This mechanism has been employed for successfully predicting the structure of CH4–NH3 and nitro-methane flames. Because of comprehensive validation with experimental data over a range of conditions, this model is recently seeing wider use and is being substituted in some instances in place of the GRI-Mech 3.0 mechanism (Hansen and Glarborg, 2010). The combustion characteristics of near-stoichiometric NH_3-air mixtures have previously been modelled at elevated pressure and temperature conditions using a derivative of the Konnov mechanism in a flat, freely propagating flame model (Duynslaegher et al., 2009). Results indicate that both equivalence ratio and compression ratio have a substantial effect on the laminar burning velocity and the adiabatic flame temperature. Lee et al., 2010, have evaluated the unstretched laminar burning velocities and stretch effects for laminar, premixed H_2–NH_3–air flames in a freely propagating spherical configuration.

In the present work, a laminar premixed jet flame has been considered, since it is more convenient for a range of subsequent studies. Numerical laminar flame speeds for premixed H_2–NH_3–air jet flames are compared and validated with experimental measurements using the one-dimensional, laminar, freely propagating flame conditions. The accuracy of the current computational approach as well as each chemical mechanism is evaluated for various conditions.

COMPUTATIONAL MODELLING

A one-dimensional, laminar, freely propagating flame model is employed in CHEMKIN package with GRI-Mech 3.0 for predicting laminar flame speeds. Such flames, which are assumed to be free from external instabilities and wall effects, represent an idealized model for conducting fundamental studies. It is worth noting that, the GRI-Mech 3.0 has well established for predicting flame structure of pure CH_4 or CH_4 mixtures with other species such as H_2 and CO, among others.

A freely propagating adiabatic, premixed, unstretched planar flame was simulated by using PREMIX (Kee et al., 1985), a steady laminar one-dimensional flame code. PREMIX uses a hybrid time integrating/ Newton iteration technique to solve the steady state mass, species and energy conservation equations and can simulate the propagating flame. Equations were solved

2

by using the TWOPNT, a boundary value problem solver in the CHEMKIN package (Kee et al., 1989). Also built in the CHEMKIN package are a transport property processor and a gas-phase interpreter, which provide the species transport properties and process the chemical reaction mechanism. One of the critical elements for simulation is the proper reaction mechanism that can describe the essential fundamental reaction paths followed by the overall reaction. GRI-MECH is an optimized detailed chemical reaction mechanism for the calculation of natural gas chemical reaction process and the latest version is GRI-MECH 3.0, which consists of 325 elementary chemical reactions with associated rate coefficient expressions and thermo chemical parameters for 53 species. It includes the detailed combustion reaction mechanism for hydrogen. The ranges of GRI-MECH 3.0 are 1000 to 2500 K in temperature, 10 Torr to 10 atm in pressure and 0.1 to 5.0 in equivalence ratio. The initial flow rate of the unburned mixture was chosen equal to 0.04 g/cm^{2}s, according to the measurement of stoichiometric methane/air flame speed by Egolfopoulos et al., 1989. To start the iteration the temperature profile estimation obtained by Van Maaren et al., 1994, for a stoichiometric methane/air flame was adopted, as suggested by Uykur et al., 2001. The temperature profile resulting from the first simulation step was used for the next step. At the inlet boundary temperature, 298 K, pressure, 0.1 MPa, and composition of the unburned mixture were assigned. At the exit boundary, it was specified that all gradients vanish. It is observed that by using adaptive grid parameters GRAD=0.02 and CURV=0.1, the burning velocity obtained is grid independent. The length of calculations have been regarded 2 cm before the spot of reaction or generally equal to 12 cm. The conservation of mass is expressed by the general continuity equation as follows:

$$\frac{\partial \rho}{\partial t} + \nabla . (\rho u) = 0 \tag{1}$$

Where, ρ is the mixture mass density and u the gas mixture velocity. The conservation of momentum, with no body forces other than gravity, is covered by,

$$\frac{\partial \rho u}{\partial t} + \nabla . (\rho u u) = \nabla . \Pi + \rho g \tag{2}$$

Where Π is the stress-tensor, and g is the acceleration due to gravity. The stress-tensor consists of a hydrodynamic and viscous part: $\Pi = -pI + \tau$ in which p is the pressure, I the unit tensor and τ the viscous stress-tensor. The equation describing the conservation of energy is written in terms of specific enthalpy h,

$$\frac{\partial \rho h}{\partial t} + \nabla . (\rho u h) = \frac{\partial p}{\partial t} + u . \nabla p + \tau : (\nabla u) - \nabla . q \tag{3}$$

Where q is the total heat flux. The term $\tau : (\nabla u)$ represents the enthalpy production due to viscous effects. When chemical reactions are to be considered, conservation equations for the species mass fractions Y_i are used. They are defined as $Y_i = \rho_i / \rho$ with ρ_i the density of species i. The density of the mixture ρ is related to the density of the various species by $\rho = \sum_{i=1}^{N_s} \rho_i$ with N_s the number of species. This leads to a conservation equation for every species mass fraction in the mixture,

$$\frac{\partial \rho Y_i}{\partial t} + \nabla . (\rho u Y_i) + \nabla . (\rho U_i Y_i) = \dot{\omega}_i, \qquad i \epsilon [1, N_s] \tag{4}$$

With U_i is the diffusion velocity of species i. The chemical source term $\dot{\omega}_i$ in this equation, is characteristic for the reactive nature of the flow. Note that Eq. (4) together with the continuity Eq. (1) gives an over-complete system, so instead of N_s only $N_s - 1$ equations in Eq. (4) have

to be solved. The mass fraction of one of the species can be computed using the following constraint,

$$\sum_{i=1}^{N_s} Y_i = 1 \tag{5}$$

An abundant species, e.g. nitrogen, is commonly chosen for this species. By definition, chemical reactions are mass conserving, so therefore the following relations hold:

$$\sum_{i=1}^{N_s} \rho Y_i U_i = 0$$

$$\sum_{i=1}^{N_s} \dot{\omega}_i = 0 \tag{6}$$

Finally, state equations are needed to complete the set of differential equations (2) – (4). The first state equation introduces the specific enthalpy h as a function of temperature T. This relation is given by,

$$h = \sum_{i}^{N_s} Y_i\, h_i \ \text{ with } \ h_i = h_i^{ref} + \int_{Tref}^{T} c_{p_i}(T)dT \tag{7}$$

and holds for perfect gases. In this equation h_i represents the enthalpy of species i and h_i^{ref} the formation enthalpy of species i at a reference value for the temperature T^{ref} and c_{p_i} the specific heat capacity at constant pressure of species i. The mixture heat capacity is defined by,

$$c_p = \sum_{i=1}^{N_s} Y_i\, c_{p_i} \tag{8}$$

The species heat capacity c_{p_i} is commonly tabulated in polynomial form. In most combustion problems, the mixture and its components are considered to behave as perfect gases. The ideal-gas law relates the density, temperature and pressure to each other by,

$$\rho = \frac{p\bar{M}}{RT} \tag{9}$$

With R the universal gas constant and $\bar{M}$ the mean molar mass. This $\bar{M}$ can be determined from,

$$\bar{M} = \left(\sum_{i=1}^{N_s} \frac{Y_i}{M_i} \right)^{-1} \tag{10}$$

Where M_i is the molar mass of species i.

RESULTS

Flame speeds are measured for each flame condition for equivalence ratios from 0.5 to 1.1 with flame speed predictions from a one-dimensional, laminar, freely propagating flame model in CHEMKIN-II package. The obtained results are then compared with flame speed predictions Kumar and Meyer, 2013, experimental study. The models are at standard temperature and pressure.

H$_2$-air Flames   Fig. 1 shows the variations of the calculated laminar flame speed with increasing equivalence ratio and its comparison with experimental measurements of Kumar and Meyer. The flame speed predictions experimental data, and GRI-MECH 3.0 mechanisms follow similar trends and match closely with measured flame speeds for equivalence ratios from 0.5 to 0.9. It is notable that the current numerical data agree closely with experimental values of Kumar and Meyer, however, the experimental data are higher than the predictions at higher equivalence ratios. This discrepancy can be attributed to the assumption of an adiabatic flame for the one-dimensional, laminar, freely propagation flame model.
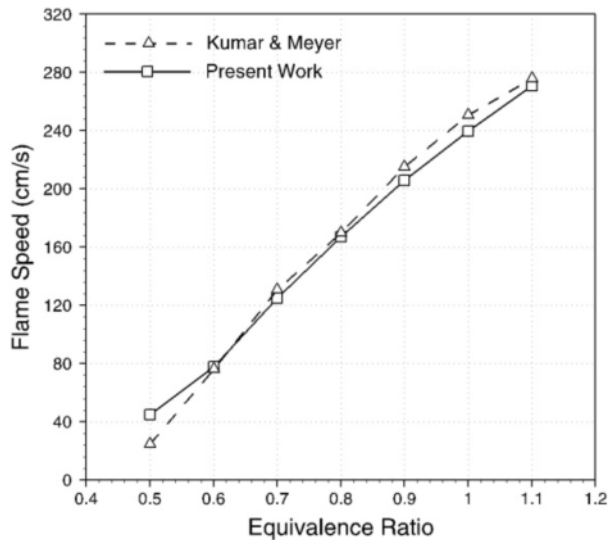

Figure 1. Comparison of computed and measured laminar flame speed variations with equivalence ratio for NH$_3$ addition at 0% by energy in H$_2$
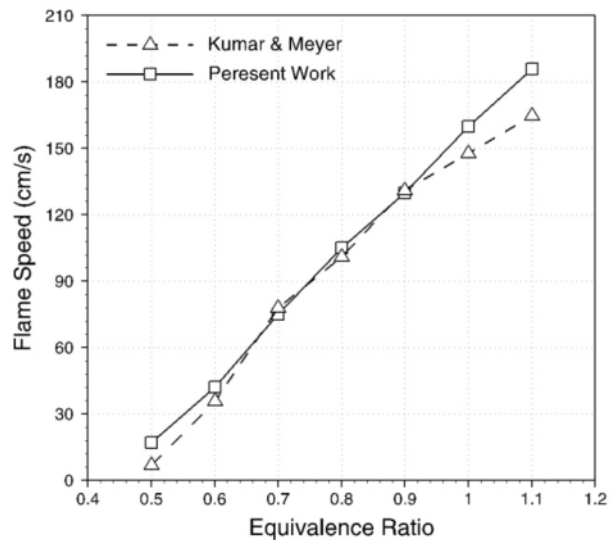
Figure 2. Comparison of computed and measured laminar flame speed variations with equivalence ratio for NH$_3$ addition at 20% by energy in H$_2$

H$_2$–NH$_3$–air Flames

NH$_3$ Addition 20% by Energy in H$_2$.   Variations in numerically calculated through GRI-MECH 3.0 mechanisms laminar flame speeds with respect to equivalence ratio are presented in Fig. 2. The computed flame speed for E%NH$_3$ = 20 increases gradually with improving equivalence ratio from 17 cm/s at φ = 0.5 to 186 cm/s at φ = 1.1. It can also be observed that the flame speed predictions by GRI-MECH 3.0 mechanisms are in close agreement with the Kumar and Meyer experimental data and both values follow the same upward trend.

NH$_3$ Addition 50% by Energy in H$_2$.   Fig. 3 illustrate the computation and measurement values of laminar flame speed as a function of equivalence ratio for E%NH$_3$ = 50. The measured flame speeds increase from 12 to 54 cm/s as equivalence ratio increases from 0.55 to 1.1. These are somewhat difference than Kumar and Meyer, who reported unstretched flame speeds of 1, 27 and 53.5 cm/s at equivalence ratios 0.6, 0.8 and 1.1 respectively, for E%NH$_3$ = 50 in a spherical propagating flame. Given the nearly six-fold drop in flame speed from E%NH$_3$ of 0 to 50 and differences in heat losses between the two flame configurations, this agreement is roughly reasonable.

NH$_3$ Addition 80% by Energy in H$_2$.   For the case of E%NH$_3$ = 80, the measured flame speeds for various equivalence ratios are demonstrated in Fig. 4. The flame speeds increase gently from 3.1 to 11 cm/s for equivalence ratio changes from 0.5 to 0.9. This is followed by a steep

increase from 0.9 to 1.1, reaching a peak flame speed of 16 cm/s. The unstretched laminar flame speeds measured by Kumar and Meyer for case $E\%NH_3 = 80$ and at equivalence ratios 0.6, 0.8 and 1.0 are 1.7, 6.8 and 9.7 cm/s, respectively.
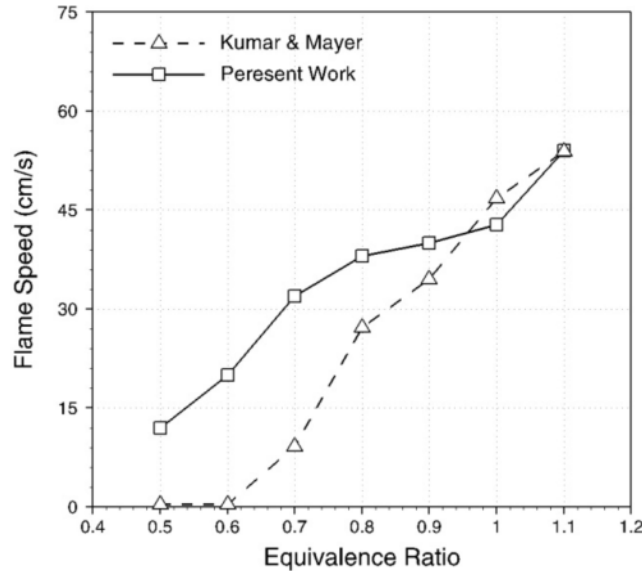
Figure 3. Comparison of computed and measured laminar flame speed variations with equivalence ratio for NH_3 addition at 50% by energy in H_2
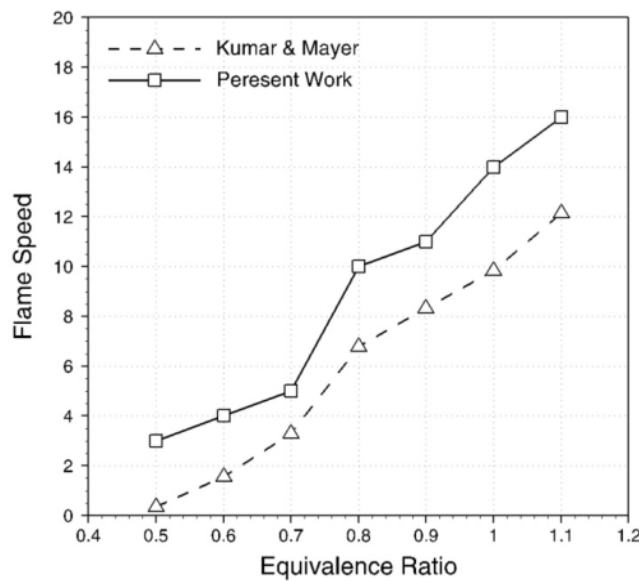
Figure 4. Comparison of computed and measured laminar flame speed variations with equivalence ratio for NH_3 addition at 80% by energy in H_2

Effects of Radicals on Flame Speed From the flame speed analysis in the previous section, it is clear from Figs. 2–4 that the heat losses reduce the laminar flame speeds of the fuel–air mixtures. Heat loss from the flame reduces the flame temperature and, thereby, lowers the rate of radical formation reactions. To investigate the effects of heat loss on radical species and flame speed in the CHEMKIN models, the concentration profiles of H, O and OH radicals are plotted for adiabatic models in Fig. 5 at an equivalence ratio of 1.0 for $E\%NH_3 = 50$.
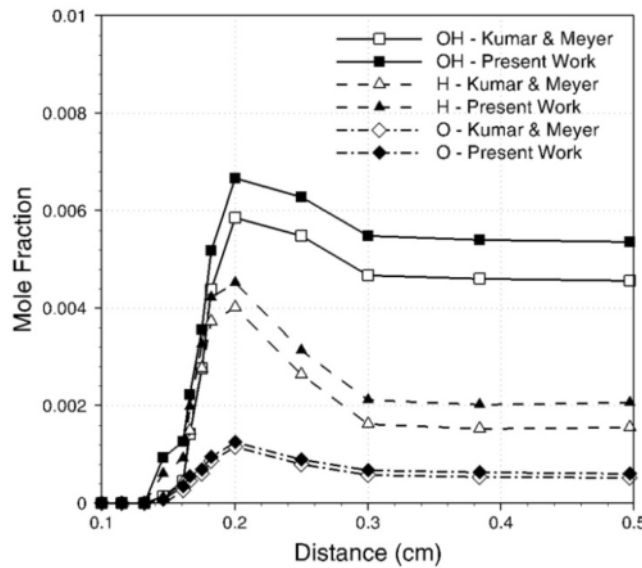
Figure 5. Mole-fraction profiles of H, O, and OH radicals at $\varphi = 1.0$ for case $E\%NH_3 = 50$, NH_3 addition at 80% by energy in H_2

To further investigate the effects of reduced radical concentrations on the rate of NH_3 decomposition at different equivalence ratios, the mole fractions of H, O and OH radicals are plotted in Fig. 6 for $E\%NH_3 = 50$. As shown in Figs. 5 and 6, significant changes in OH and H radicals could lead to significant changes in flame speed with heat losses and changes in equivalence ratio. In particular, because OH has the greatest effect on NH_3 decomposition, the relatively high mole fraction of OH radicals leads to a higher flame speed at $\varphi = 0.6$ and a greater increase in flame speed at higher equivalence ratio. Ultimately, the comparison of computation flame speed data at $\varphi = 0.6$ and $\varphi = 1.0$ is shown in Fig. 7.
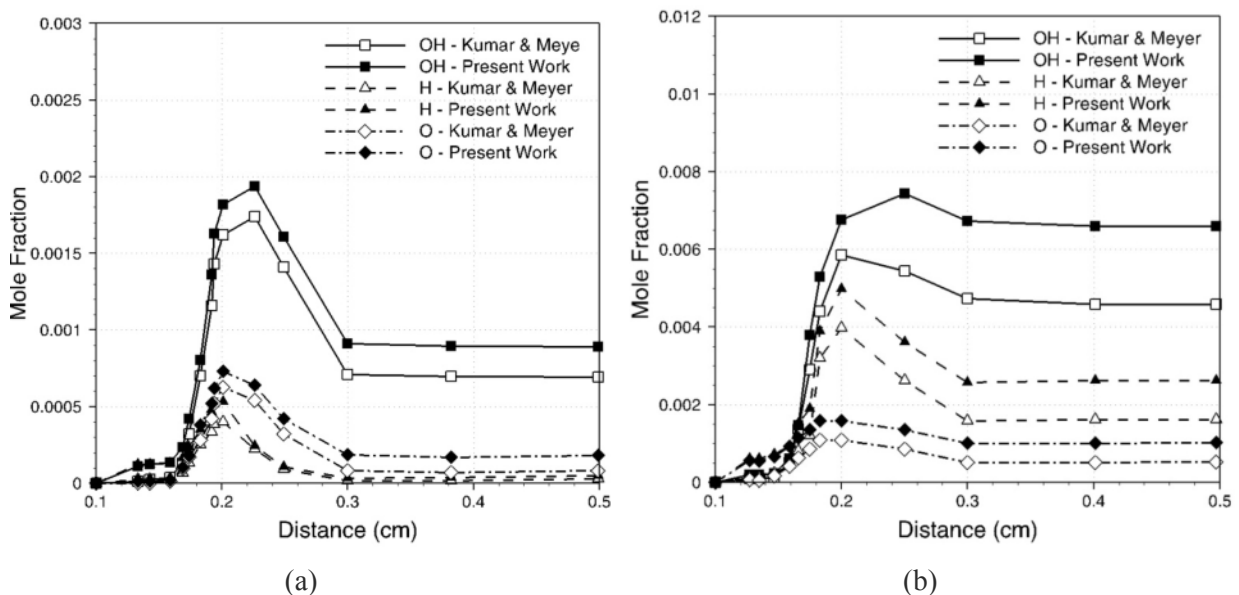

(a)

(b)

Figure 6. Mole fraction profiles of H, O, and OH at (a) $\varphi = 0.6$ and (b) $\varphi = 1.0$ for case $E\%NH_3 = 50$, NH_3 addition at 80% by energy in H_2
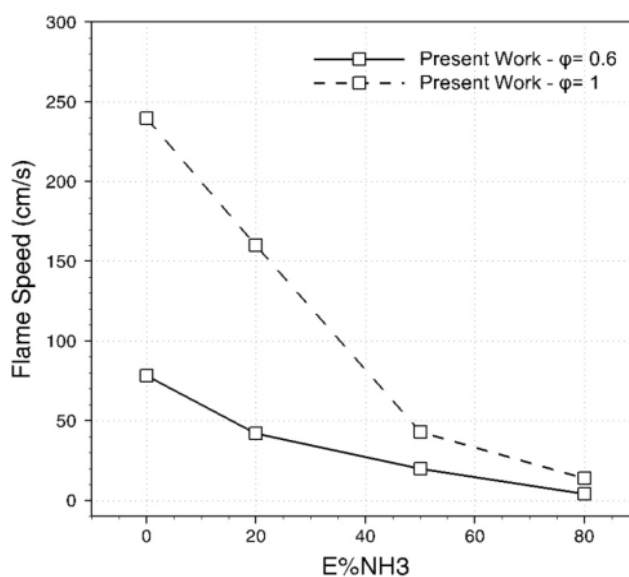
Figure 7. Comparison of computation flame speed data at $\varphi = 0.6$ and $\varphi = 1.0$

CONCLUSIONS

Flame speed calculations are performed for H_2–NH_3–Air mixtures in a laminar jet flame configuration, and acquired data are compared with flame speed measurements of Kumar and Meyer. One-dimensional, laminar, freely propagating flame speed has been modelled in the CHEMKIN package. The equivalence ratio varied from 0.5, lean conditions, to 1.1, reach conditions, and also cases included NH_3 as a percent of the energy in H_2 of E%$NH_3 = 0$ (pure H_2–air), 20, 50 and 80. The results showed that laminar flame speed predictions using of GRI-MECH 3.0 are in good agreement with experimental values of Kumar and Meyer. It is also verified that the radical pool of OH, H, and O plays an important role in controlling the total rate of decomposition of NH_3, with OH having a more significant impact. From the current study, it is revealed that the radical mole fractions have strong implications on the predicted flame speeds. Similarly, the differences in radical mole fractions may be consequential for the NO formation in the flame. Hence, follow-on work will include investigation of the effects of radical species on the NO formation rates in H_2–NH_3–air flames.

REFERENCES

Bian, J. [1991], Experimental study of the formation of nitrous and nitric oxides in H_2-O_2-Ar flames seeded with NO and/or NH_3, *Symposium (International) Combustion*, Vol. 23, No. 1, pp. 379-386.

Duynslaegher, C., Jeanmart, H. and Vandooren, J. [2009], Flame structure studies of premixed ammonia/hydrogen/oxygen/argon flames: experimental and numerical investigation, *Proceedings of the Combustion Institute*, Vol. 32, No. 1, 1277-1284.

Duynslaegher, C., Jeanmart, H. and Vandooren, J. [2009], Use of ammonia as a fuel for SI engine, *Proceedings of the European Combustion Meeting*, pp. 1-6.

Egolfopoulos, F.N., Cho, P. and Law, C.K. [1989], Laminar flame speeds of methane/air mixtures under reduced and elevated pressures, *Combustion and Flame*, Vol. 76, No. 3-4, pp. 375-391.

Hansen, S. and Glarborg, P. [2010], Simplified model for re-burning chemistry, *Energy and Fuel*, Vol. 24, No. 8, pp. 4185-4192.

Kee, R.J., Grcar, J.F., Smooke, M.D. and Miller, J.A. [1985], PRMIX: a FORTRAN program for modeling steady laminar one-dimensional premixed flames, Sandia National Laboratory, SAND Report 85-8240.

Kee, R.J., Rupley, F.M. and Miller, J.A. [1989], CHEMKIN-II: a FORTRAN chemical kinetics package for the analysis of gas-phase chemical kinetics, Technical Report SAND, Sandia National Laboratories 89-8009.

Konnov, A.A. [2009], Implementation of the NCN pathway of prompt-NO formation in the detailed reaction mechanism, *Combustion and Flame*, Vol. 156, No. 11, pp. 2093-2105.

Kumar, P. and Meyer, T.R. [2013], Experimental and modelling study of chemical-kinetics mechanisms for H_2–NH_3–air mixtures in laminar premixed jet flames, *Fuel*, Vol. 108, pp. 166-176.

Lee, J.H., Kim, J.H., Park, J.H. and Kwon, O.C. [2010], Studies on properties of laminar premixed hydrogen-added ammonia/air flames for hydrogen production, *International Journal of Hydrogen Energy*, Vol. 35, No. 3, pp. 1054-1064.

Lee, J.H., Lee, S.I. and Kwon, O.C. [2010], Effects of ammonia substitution on hydrogen/air flame propagation and emissions, *International Journal of Hydrogen Energy*, Vol. 35, No. 20, pp. 11332-11341.

Mendiara, T. and Glarborg, P. [2009], Ammonia chemistry in oxy-fuel combustion of methane, *Combustion and Flame*, Vol. 156, No. 10, pp. 1937-1949.

Miller, J.A. and Bowman, C.T. [1989], Mechanism and modelling of nitrogen chemistry in combustion, *Progress in Energy and Combustion Science*, Vol. 15, No. 4, pp. 287-338.

Reiter, A.J. and Kong, S.C. [2011], Combustion and emissions characteristics of compression-ignition engine using dual ammonia-diesel fuel, *Fuel*, Vol. 90, No. 1, pp. 87-97.

Shmakov, A.G., Korobeinichev, O.P., Rybitskaya, I.V., Chernov, A.A., Knyazkov, D.A., Bolshova, T.A. and Konnov, A.A. [2010], Formation and consumption of NO in H2/O2/N2 flames doped with NO or NH3 at atmospheric pressure, *Combustion and Flame*, Vol. 157, No. 3, pp. 556-565.

Tian, Z., Li, Y., Zhang, L., Glarborg, P. and Qi, F. [2009], An experimental and kinetic modelling study of premixed NH_3/CH_4/O_2/Ar flames at low pressure, *Combustion and Flame*, Vol. 156, No. 7, pp. 1413-1426.

Uykur, C., Henshaw, P.F., Ting, D.S.K. and Barron, R.M. [2001], Effects of addition of electrolysis product on methane/air premixed laminar combustion, *International Journal of Hydrogen Energy*, Vol. 26, No. 3, pp. 265-273.

Van Maaren, A., Thung, D.S. and De Goey L.P.H. [1994], Measurement of flame temperature and adiabatic burning velocity of methane/air mixtures, *Combustion Science and Technology*, Vol. 96, No. 4, pp. 327-344.

Zamfirescu, C. and Dincer, I. [2009], Ammonia as a green fuel and hydrogen source for vehicular applications, *Fuel Process Technol*ogy, Vol. 90, No. 5, pp. 729-37.